Journal of Microbiological Methods 98 (2014) 50–58

Contents lists available at ScienceDirect

Journal of Microbiological Methods

journal homepage: www.elsevier.com/locate/jmicmeth

Rapid antibiotic susceptibility phenotypic characterization of *Staphylococcus aureus* using automated microscopy of small numbers of cells☆,☆☆

Connie S. Price [a], Shelley E. Kon [a,1], Steven Metzger [b,*]

[a] Denver Health Medical Center, Division of Infectious Diseases Medicine, Denver, CO 80204, USA
[b] Accelerate Diagnostics Inc., Denver, CO 80221, USA

ARTICLE INFO

Article history:
Received 21 October 2013
Received in revised form 18 December 2013
Accepted 18 December 2013
Available online 4 January 2014

Keywords:
Antibiotic susceptibility testing
Rapid AST
Antibiotic resistance
Phenotypic detection
MRSA
Staphylococcus aureus

ABSTRACT

Staphylococcus aureus remains a leading, virulent pathogen capable of expressing complex drug resistance that requires up to 2–4 days for laboratory analysis. In this study, we evaluate the ability of automated microscopy of immobilized live bacterial cells to differentiate susceptible from non-susceptible responses of *S. aureus* isolates (MRSA/MSSA, clindamycin resistance/susceptibility and VSSA/hVISA/VISA) to an antibiotic based on the characterization of as few as 10 growing clones after 4 h of growth, compared to overnight growth required for traditional culture based methods. Isolates included 131 characterized CDC isolates, 3 clinical isolates and reference strains. MRSA phenotype testing used 1 h of 1 μg/mL cefoxitin induction followed by 3 h of 6 μg/mL cefoxitin. Clindamycin susceptibility testing used 1 h of induction by 0.1 μg/mL erythromycin followed by 3 h of 0.5 μg/mL clindamycin. An automated microscopy system acquired time-lapse dark-field images, and then computed growth data for individual immobilized progenitor cells and their progeny clones while exposed to different test conditions. Results were compared to concurrent cefoxitin disk diffusion and D-test references. For CDC organisms, microscopy detected 77/77 MRSA phenotypes and 54/54 MSSA phenotypes, plus 53/56 clindamycin-resistant and 75/75 clindamycin susceptible strains. Automated microscopy was used to characterize heterogeneous and inducible resistance, and perform population analysis profiles. Microscopy-based hVISA population analysis profiles (PAPs) were included as an extended proof of concept, and successfully differentiated VSSA from hVISA and VISA phenotypes compared to plate-based PAP.

1. Introduction

Staphylococcus aureus is a leading cause of serious infection in both the hospital and the community (Landrum et al., 2012; Klevens et al., 2007). Methicillin-resistant *S. aureus* (MRSA) has evolved as a leading cause of nosocomial infections worldwide and has also emerged as a major resistance phenotype in community-acquired infections (Chambers and Deleo, 2009). MRSA strains inherently resist essentially all β-lactam antibiotics, which make up the largest, most effective, and most widely used class of antibiotics. Clinical MRSA strains are frequently multi-drug resistant (MDR) and may express numerous virulence factors (Skrupky et al., 2009), making staphylococcal infections increasingly difficult to treat. *S. aureus* can have additional types of antibiotic resistance including resistance to clindamycin and reduced susceptibility to vancomycin.

Antimicrobial susceptibility testing (AST) is essential to assure appropriate antibiotic choice in treating infection, but typically requires 2–4 days to produce results. Guidelines (Muscedere et al., 2008; Liu et al., 2011) recommend starting empiric broad-spectrum antibiotic therapy within 1–3 h of the time that a critically ill patient exhibits signs of a potentially severe infection. Because of widespread antibiotic resistance, the patient is thus at risk of receiving inadequate therapy during the wait for laboratory results (Ibrahim et al., 2000; Iregui et al., 2002).

Automated microscopy of immobilized individual live bacterial cells is an innovative rapid phenotyping method for AST that analyzes the properties of a small number of cells to infer the phenotypic response of an entire population in hours compared to overnight culturing methods. The first purpose of this study is to evaluate the performance of automated microscopy to detect the MRSA phenotype and clindamycin resistance using induction-based assays on small numbers of cells compared to conventional AST confirmatory methods. Secondly, the ability of the automated microscopy method to characterize heteroresistant and inducible

☆☆ Findings from preliminary studies related to this study were previously presented in part at the American Society for Microbiology 2008 and 2011 General Meetings (Metzger et al., 2008, 2011).

* Corresponding author at: Accelerate Diagnostics Inc., 3950 S. Country Club Rd., Ste. 470, Tucson, AZ 85714, USA. Tel.: +1 520 365 3100; fax: +1 520 269 6580.
E-mail address: smetzger@axdx.com (S. Metzger).
[1] Present address: Georgetown University Hospital, Washington, D.C., 20007, USA.

0167-7012/$ – see front matter © 2014 The Authors. Published by Elsevier B.V. All rights reserved.
http://dx.doi.org/10.1016/j.mimet.2013.12.021

strains was evaluated, including the time necessary to reveal a phenotypic response as well as the minimum number of cells required. As an extended proof of principle, a microscopy-based population analysis profile (PAP) to differentiate heterogeneous vancomycin intermediate *S. aureus* (hVISA) and VISA strains from vancomycin susceptible *S. aureus* (VSSA) was evaluated, as this is the best-known use of PAP currently.

2. Materials and methods

2.1. S. aureus isolates

S. aureus isolates included quality control strains specified by the CLSI for the purposes of susceptibility testing (CLSI, 2009): ATCC® 43300 MRSA, ATCC 29213 and 27659 methicillin susceptible *S. aureus* (MSSA), BAA-977 clindamycin (CLI) inducible resistance, BAA-976 CLI susceptible, Mu50/ATCC 700699 VISA, and Mu3/ATCC 700698 hVISA (ATCC, Manassas, VA). The Washington University School of Medicine (St. Louis, MO) Barnes-Jewish Hospital provided three *S. aureus* clinical isolates (1-3C, 1-4C, and 1-6I) that showed growth on 3 μg/mL vancomycin screening agar. The United States Centers for Disease Control and Prevention (CDC, Atlanta, GA) provided 131 characterized *S. aureus* isolates that expressed borderline oxacillin resistance and contained 78 *mecA* positive strains and 53 *mecA* negative strains (Swenson et al., 2007). Thirty-eight of the CDC strains were D-test positive for inducible CLI resistance, 18 strains expressed constitutive CLI resistance, and 75 strains were CLI susceptible (Table 1).

Each strain was recovered from −80 °C frozen storage and subcultured on sheep's blood agar (Becton Dickinson, Sparks, MD). Five to ten colonies selected from a fresh overnight subculture plate were suspended by vortexing in tryptic soy broth (Becton Dickinson) and incubated for 2 h at 35 ± 2 °C to achieve log phase growth. The bacterial suspension was centrifuged (12,000 × *g* for 4 min), washed in 1 mM L-histidine buffer at a pH of 7.2, and resuspended in a low ionic strength electrokinetic buffer containing 10 mM L-DOPA and 1 mM L-histidine at a pH of 7.0 (Accelerate Diagnostics, Tucson, AZ) to create an inoculum of approximately 1×10^6 CFU/mL.

2.2. Bacterial immobilization

Automated microscopy tests were performed in a custom disposable multichannel fluidic cassette containing 32 independent fluidic channels, with each channel having its own independent inlet and outlet ports for fluid exchange by pipetting (Fig. 1). Each fluidic channel consisted of a rectangular conduit formed by a die-cut double-adhesive polyester mask approximately 300 μm thick enclosed by transparent top and bottom covers. The top cover was also polyester, while the bottom cover consisted of a standard 1 × 3 inch glass microscope slide. The top and bottom surfaces of each fluidic channel had a transparent, electrically conductive coating of indium tin oxide. The bottom surface had an additional coating of poly-L-lysine. Bacteria were negatively-charged in the electrokinetic buffer.

After pipetting 20–30 μL of bacterial inoculum into each independent fluidic channel, a 5-min low voltage electrical field applied across the two indium tin oxide layers concentrated individual cells in a random dispersion on the bottom surface. After the current was stopped, the negatively-charged cells remained adherent to the poly-cationic poly-L-lysine layer through electrostatic binding. This allowed the operator to pipette test solutions into each fluidic channel to replace the electrokinetic buffer without detaching the cells. All antibiotic test solutions were prepared using cation-adjusted Mueller–Hinton broth (Becton Dickinson).

Table 1
Characteristics of CDC *S. aureus* isolates.

	mecA status	Cefoxitin disk diffusion result		D-test result		
		MRSA	MSSA	cCLI-R[a]	iCLI-R[b]	CLI-S[c]
n = 131	78 positive	77	1	17	27	34
	53 negative	0	53	1	11	41

[a] cCLI-R = constitutive clindamycin resistance.
[b] iCLI-R = inducible clindamycin resistance.
[c] CLI-S = clindamycin susceptible.

2.3. Automated microscopy

Immobilized bacteria were viewed using a custom microscopy instrument (Accelerate Diagnostics Inc., Tucson, AZ) that consisted of an assembly with an inverted IX-71 microscope (Olympus America, Inc., Center Valley, PA) adapted with commercially available accessories and a 20 × 0.45 NA objective lens that viewed each fluidic channel from below. Transmitted dark-field illumination was generated using a halogen light source (Olympus). A 12-bit monochrome MicroFire camera (Olympus) with a 1600 × 1200 pixel frame size captured dark-field time-lapse images in each fluidic channel at 10-min intervals over the antibiotic exposure period. Each field of view covered an area of 592 × 444 μm^2 and the observation zone accommodated up to 42 fields of view per fluidic channel (Fig. 1). A PC running custom experiment control software (Accelerate Diagnostics) executed all automated operations. An XY stage (Prior Scientific, Cambridge, UK) driven by stepper motors enabled cassette scanning for synchronous image acquisition. A heated enclosure maintained the entire instrument setup at 35 ± 2 °C.

2.4. Image analysis

Once collected, the dark-field image sequences were analyzed offline using custom image analysis software (Accelerate Diagnostics). The software assigned unique individual spatial XY coordinates to each immobilized progenitor cell within each fluidic channel. As each progenitor cell grew into a clone of daughter cells, the assigned coordinates enabled the software to locate each individual growing clone throughout a series of time-lapse images. The software measured each clone's intensity as a metric of clone mass in each image. Analysis algorithms calculated a growth probability score for each growing clone derived from coefficients of a cubic polynomial fitted to a plot of the natural log of the clone mass *vs.* time. The growth probability score transformed the shape of each curve into a numerical score ranging between 0 and 1 that represented the probability of the clone continuing to grow, to arrest, or to lose mass (lyse). The slope of the cubic polynomial was used to calculate instantaneous division rates for individual clones at specified time points. For AST classification, a growth analysis algorithm multiplied the growth probability for each clone by its 4 h endpoint integrated intensity (which is proportional to total cell count at 4 h) and summed for all clones. This weighted growth probability was then divided by the summed intensity of all clones to derive an AST probability score for each isolate.

2.5. MRSA phenotype detection

Triplicate automated microscopy runs were performed on 131 CDC borderline isolates for MRSA phenotype detection. For each test, a separate growth control channel contained the same growth medium without any drug. A second channel used 1 μg/mL cefoxitin for 1 h of induction followed by 3 h of challenge with 6 μg/mL cefoxitin. A third channel used drug-free medium for 1 h of growth followed by 3 h of challenge with 6 μg/mL cefoxitin (no induction) as a reference to assess the magnitude of induction effects. A fourth channel used 1 μg/mL cefoxitin for 1 h followed by 3 h in drug-free medium as a control. Images were obtained every 10 min for the 3 h challenge period. AST probability scores above or below the criterion level of 0.4 classified an isolate as MRSA or MSSA, respectively. Concurrent standard CLSI

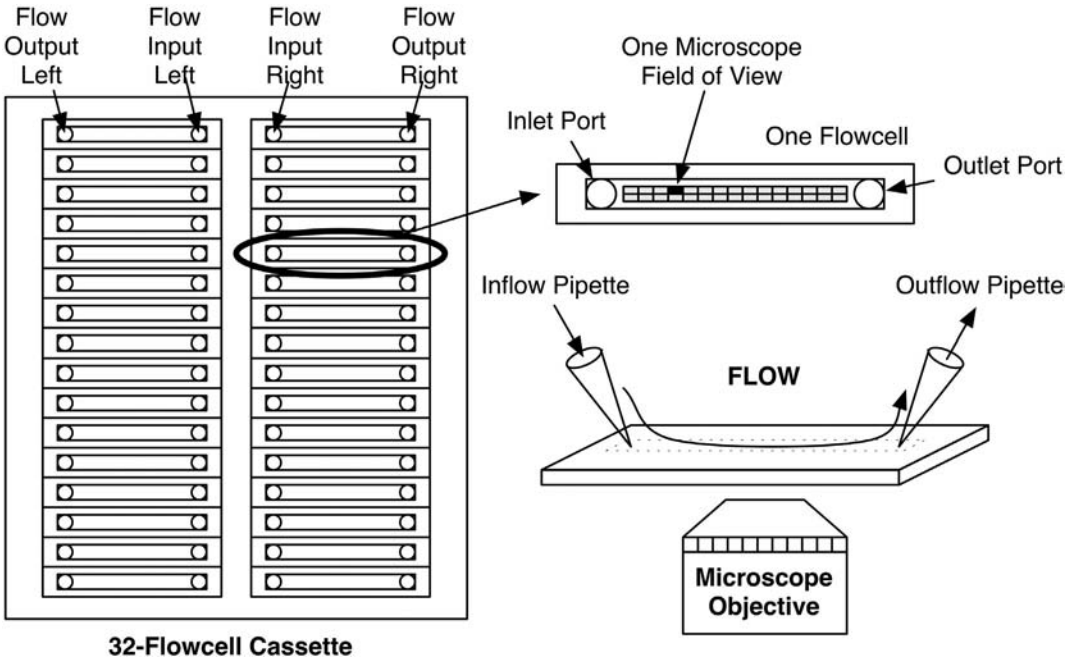

Fig. 1. Diagram of 32-channel cassette showing detail of individual fluidic channel and microscope fields of view. Fluid exchange occurs using pipette inflow and outflow ports, and image capture is performed by an inverted microscope positioned beneath the bottom surface of the fluidic channel.
Reprinted from Diagnostic microbiology and infectious disease, S. Metzger, R.A. Frobel, W.M. Dunne, Jr., Rapid simultaneous identification and quantitation of *Staphylococcus aureus* and *Pseudomonas aeruginosa* directly from bronchoalveolar lavage specimens using automated microscopy, in press. Copyright 2012, with permission from Elsevier.

cefoxitin disk diffusion (FOX-DD) tests provided the reference methodology (Howden et al., 2010).

2.6. Clindamycin resistance detection

Triplicate automated microscopy runs were performed on 131 CDC borderline isolates to characterize clindamycin resistance. For each test, a separate growth control channel contained the same growth medium without any drug. A second channel used 0.1 μg/mL erythromycin for 1 h of induction followed by 3 h of challenge with 0.5 μg/mL clindamycin (Weisblum et al., 1971). A third channel used drug-free medium for 1 h of growth followed by 3 h of challenge with 0.5 μg/mL clindamycin (no induction) as a reference to assess the magnitude of induction effects. A fourth channel used 0.1 μg/mL erythromycin for 1 h followed by 3 h in drug-free medium as a control. Images were obtained every 10 min for the 3 h challenge period. AST probability scores above or below the criterion level of 0.4 classified an isolate as clindamycin resistant or susceptible, respectively. Concurrent standard CLSI disk approximation induction testing with erythromycin and clindamycin disks (D-test) was used as the reference for both inducible and constitutive resistance (Howden et al., 2010).

2.7. Characterization of heterogeneous MRSA

Instantaneous division rates at 30, 90 and 180 min were calculated for all individual clones for CDC isolates BS-001 (MSSA), BS-006 (MRSA) and BS-067 (MRSA) in 6 μg/mL cefoxitin channels with 1 μg/mL cefoxitin induction step. Individual clonal division rates were plotted to generate histograms of individual clonal responses.

2.8. Characterization of inducible MRSA and clindamycin resistance

Instantaneous division rates were calculated for all individual clones for CDC isolates BS-002 (MSSA), BS-006 (MRSA) and BS-023 (inducible MRSA) in 6 μg/mL cefoxitin channels with and without 1 μg/mL cefoxitin induction step to test for inducible resistance to cefoxitin. Instantaneous division rates were calculated for all individual clones for CDC isolates BS-042 (clindamycin susceptible), BS-051 (constitutive clindamycin resistance), and BS-071 (inducible clindamycin resistance) in 0.5 μg/mL clindamycin channels with and without 0.1 μg/mL erythromycin induction step to test for inducible resistance to clindamycin. Average clonal division rates for each isolate were plotted *vs.* time to generate growth curves for comparison.

2.9. Minimum clone simulation

A computer simulation randomly picked 1, 3, 5, 10, 25 or 50 clones from each MRSA phenotype or clindamycin resistance test run and calculated the resulting average growth probability for each set of triplicate runs for each isolate. These values were used to calculate sensitivity and specificity for each isolate based on each number of clones.

2.10. Population analysis profile (PAP) by automated microscopy and plating

Six isolates (Mu50, Mu3, 1-6I, 1-4C, BS-003 and 1-3C) with vancomycin MICs ranging from 0.5 to 8 μg/mL were selected for PAP. For automated microscopy-based PAP, each isolate was placed in ten fluidic channels. Molten 0.85% agar (Becton Dickinson) at 42 °C was added to growth medium containing the following concentrations of vancomycin

		Cefoxitin Disk Diffusion: MRSA	Cefoxitin Disk Diffusion: MSSA	
Automated Microscopy	MRSA	77	0	PPV=100%
	MSSA	0	54	NPV=100%
		Sensitivity=100%	Specificity=100%	

Fig. 2. Performance characteristics of automated microscopy MRSA phenotype test compared to cefoxitin (FOX) disk diffusion for 131 CDC *S. aureus* isolates. Automated microscopy classifications are based on growth probability values from triplicate runs (MRSA ≥ 0.4 > MSSA). PPV = positive predictive value; NPV = negative predictive value.

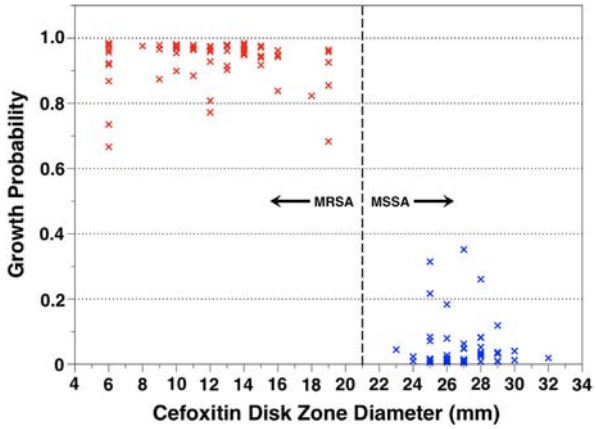

Fig. 3. Scatter plot comparing MRSA phenotype classification results for 131 CDC *S. aureus* isolates generated by automated microscopy and cefoxitin (FOX) disk diffusion. Growth probabilities are the average from triplicate automated microscopy runs.

(Sigma-Aldrich): 0, 0.01, 0.05, 0.1, 0.2, 0.4, 0.8, 1.0, 2.0, or 4.0 μg/mL. Each concentration of agar/vancomycin medium was introduced into one of the ten fluidic channels, and solidified by cooling to ambient temperature (<30 °C) prior to image acquisition. The image analyzer identified the number of growing clones that exhibited at least 4-fold gain in mass over the 4 h analysis period. Computation normalized these counts by dividing them by the total number of growing clones detected. These normalized counts were indexed between 0 and 1 and plotted *vs.* vancomycin concentration to generate microscopy-based PAPs.

An abbreviated plate-based PAP (Pfeltz et al., 2001) used 10-fold serial isolate concentrations from 1×10^1 to 1×10^8 CFU/mL pipette-dropped in duplicate onto sectors of agar plates containing 0, 0.25, 0.5, 0.75, 1, 2, 2.5, 3, 4, or 6 μg/mL vancomycin. Colonies were manually counted after 48 h of growth, and normalized and indexed plate counts were plotted *vs.* vancomycin concentration to generate plate-based PAPs. Area under the curve (AUC) was measured in all tests.

2.11. Statistical methods

Comparisons between automated microscopy and culture control methods for phenotype tests were summarized in 2 × 2 tables with calculations for sensitivity, specificity and positive and negative predictive values.

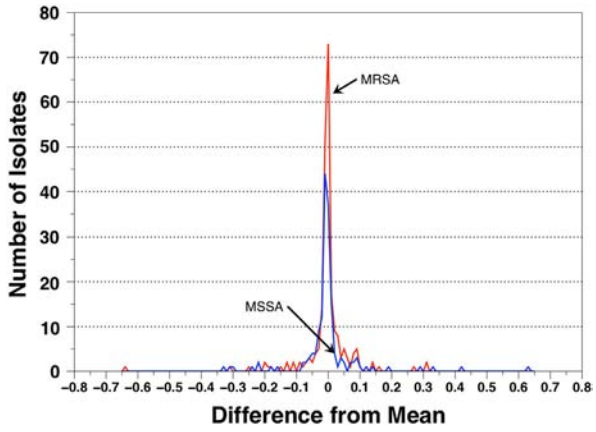

Fig. 4. Reproducibility of MRSA phenotype test. Difference from mean of automated microscopy growth probability values for triplicate runs on 131 CDC *S. aureus* isolates. Results separated by MSSA or MRSA phenotype.

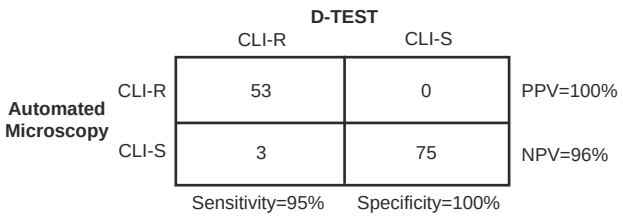

Fig. 5. Performance characteristics of automated microscopy clindamycin resistance test compared to D-test for 131 CDC *S. aureus* isolates. Automated microscopy classifications are based on growth probability values from triplicate runs (CLI-R ≥ 0.4 > CLI-S). CLI-R = clindamycin resistant; CLI-S = clindamycin susceptible; PPV = positive predictive value; NPV = negative predictive value.

3. Results

3.1. MRSA detection

Phenotype testing by automated microscopy detected 78/78 (sensitivity = 100%) CDC strains as MRSA and 57/57 (specificity = 100%) as MSSA, using cefoxitin disk diffusion phenotype testing as the reference (Figs. 2 & 3). Overall repeatability between tests on individual isolates was approximately 95% for both MRSA and MSSA strains (Fig. 4). Five MSSA strains (BS-001, BS-033, BS-036, BS-059 and BS-097) and one MRSA strain (BS-096) had discordant classifications between triplicate runs. Growth probabilities ranged from 0.003 to 0.195 below the cutoff and from 0.423 to 0.985 above the cutoff of 0.4 for the five MSSA strains. MRSA strain BS-096 had growth probabilities of 0.031 *vs.* 0.984 and 0.984 over three runs.

3.2. Clindamycin resistance detection

Automated microscopy classified 53/56 (sensitivity = 95%) as clindamycin resistant and 75/75 (specificity = 100%) CDC strains as clindamycin susceptible, using the D-test as the reference (Figs. 5 & 6). 100% of constitutive clindamycin resistance strains were detected as resistant. Two inducible clindamycin resistant strains (BS-069, BS-050) had all growth probabilities from triplicate runs below the cutoff of 0.4, classifying them as false susceptibles. Inducible clindamycin resistant strain BS-070 had one test result with a growth probability above the 0.4 cutoff (0.448), while the other two tests produced growth probabilities below the cutoff (0.206 and 0.353), classifying it as a false susceptible. Two inducible clindamycin resistant strains (BS-027 and BS-137) and one clindamycin susceptible strain (BS-132) had discordant classifications between triplicate runs. Strain BS-027 had growth probabilities of 0.088 *vs.* 0.928 and 0.895, and strain BS-137 had growth

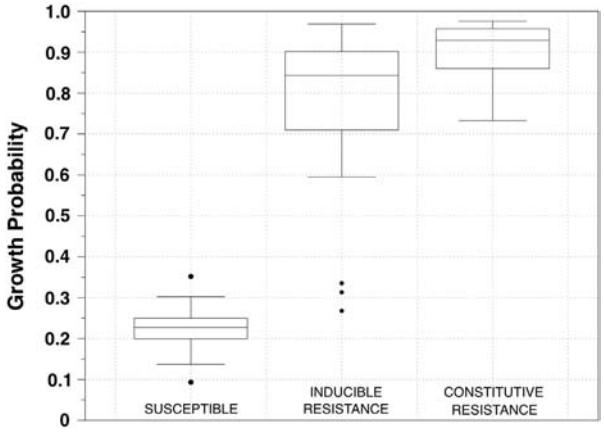

Fig. 6. Scatter plot of clindamycin phenotype classification results for 131 CDC *S. aureus* isolates generated by automated microscopy. Growth probabilities are the average from triplicate automated microscopy runs.

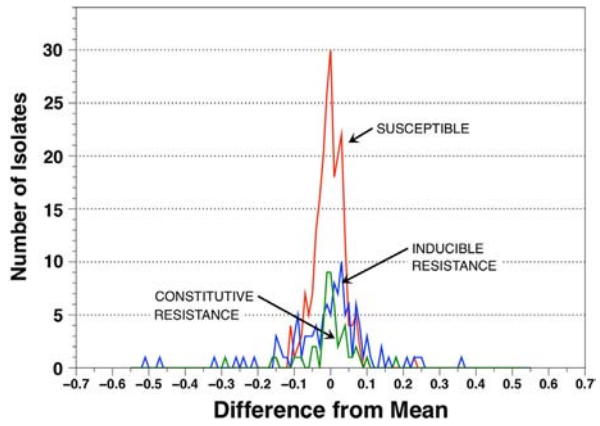

Fig. 7. Repeatability of clindamycin resistance phenotype test. Difference from mean of automated microscopy growth probability values for triplicate runs on 131 CDC *S. aureus* isolates. Results separated by phenotype.

probabilities of 0.212 *vs.* 0.895 and 0.928. Strain BS-132 had growth probabilities of 0.588 *vs.* 0.198 and 0.269. Overall repeatability between tests on individual isolates was approximately 95% for susceptible and constitutive resistant strains, and approximately 90% for inducible resistant strains (Fig. 7).

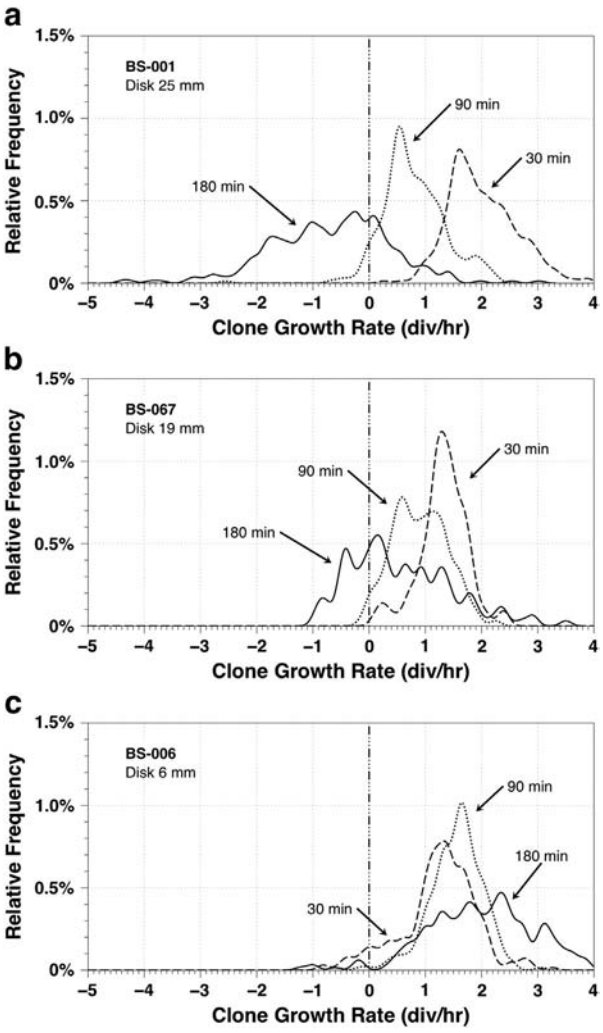

Fig. 8. Frequency distributions of clonal growth rates for *S. aureus* isolates (a) BS-001 (MSSA), (b) BS-067 (MRSA), and (c) BS-006 (MRSA). Individual clone growth rates in divisions per hour (div/h) measured during exposure to 6 μg/mL cefoxitin at 30, 90 and 180 min using automated microscopy are shown. The vertical axis represents the proportion of all clones measured, binned by division rate and smoothed for visualizing changes at different durations of drug exposure.

3.3. Heterogeneous MRSA analysis

Population analysis profiles of strains BS-001 (MSSA), BS-067 (MRSA) and BS-006 (MRSA) based on instantaneous division rates of individual clones at 30, 90 and 180 min were generated using automated microscopy of strains exposed to 6 μg/mL cefoxitin following a 1 h induction step in 1 μg/mL cefoxitin (Fig. 8). 100% of MSSA strain BS-001 clones had division rates >0 after 30 min in 6 μg/mL cefoxitin. Division rates shifted to the left with prolonged exposure, until 73% of the population division rates were <0 after 180 min, indicating susceptibility. 100% of MRSA strain BS-067 clones had division rates >0 after 30 min in cefoxitin. Division rates also shifted slightly to the left with prolonged exposure. However, 71% of the BS-067 population had division rates >0 after 180 min, indicating resistance. MRSA strain BS-006 had division rates shift to the right with prolonged exposure and 97% of the population division rates were >0 after 180 min, indicating resistance.

3.4. Characterization of inducible MRSA and clindamycin resistance

Growth curves based on the average division rates of all clones in the strain population for MSSA strain BS-002 and MRSA strains BS-006 and BS-023 are shown in Fig. 9. MSSA strain BS-002 average division rates started at ~1.4 div/h and decreased to negative values over 3 h of exposure to 6 μg/mL cefoxitin with and without prior induction with 1 μg/mL cefoxitin, indicating susceptibility. MRSA strain BS-006 starting average division rates decreased slightly from 1.3 div/h to 0.9 div/h after 1 h of exposure to 1 μg/mL cefoxitin. After 3 h of additional exposure to 6 μg/mL cefoxitin both curves showed final division rates ~1.7 div/h,

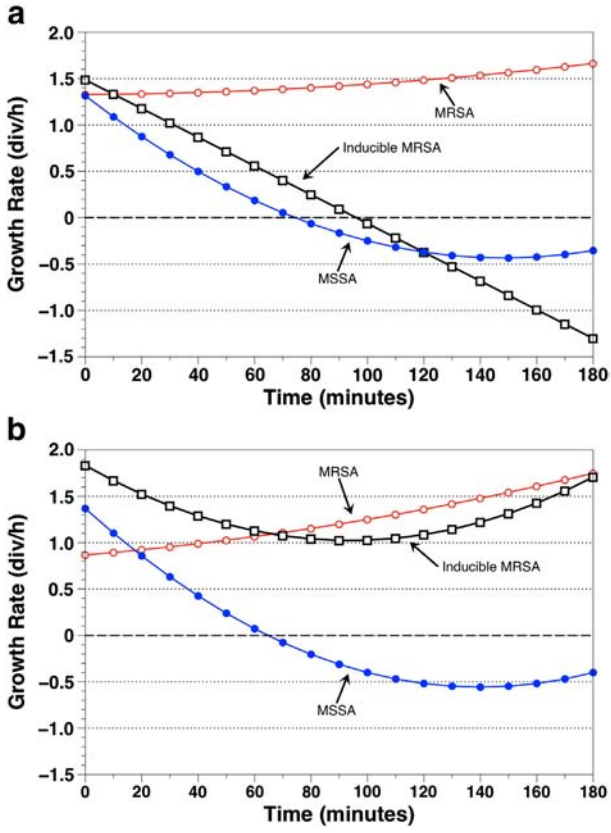

Fig. 9. Growth curves for strains BS-006 (MRSA), BS-023 (inducible MRSA) and BS-002 (MSSA) over 3 h of exposure to 6 μg/mL cefoxitin following 1 h of exposure to (a) Mueller-Hinton broth or (b) 1 μg/mL cefoxitin. The curves are based on the average division rates of all clones in the strain population.

indicating resistance. In contrast, starting average division rates for inducible MRSA strain BS-023 increased from 1.5 to 1.8 div/h upon exposure to 1 μg/mL cefoxitin for 1 h, compared to Mueller–Hinton broth alone. Without prior induction, average division rates fell to negative values after 3 h of exposure to 6 μg/mL cefoxitin. When induced with 1 μg/mL cefoxitin, BS-023 exhibited average division rates of ~1.7 div/h after 3 h of exposure to 6 μg/mL cefoxitin, indicating resistance. Growth curves for strains exhibiting clindamycin susceptibility (BS-042), constitutive clindamycin resistance (BS-051) and inducible clindamycin resistance (BS-071) based on the average division rates of all clones in the strain population are shown in Fig. 10. Strain BS-042 starting average division rates decreased from 0.9 to 0.6 div/h after 1 h of exposure to 0.1 μg/mL erythromycin, indicating erythromycin susceptibility. After 3 h of additional exposure to 0.5 μg/mL clindamycin, BS-042 division rates decreased to 0.2 div/h independent of prior induction with erythromycin, indicating susceptibility. Strain BS-051 average division rates started at ~0.9 div/h and increased to ~1.2 div/h after 3 h of exposure to 0.5 μg/mL clindamycin independent of prior induction with erythromycin, indicating resistance. Average division rates for inducible strain BS-071 decreased from 1 div/h to 0.2 div/h over 3 h of exposure to 0.5 μg/mL clindamycin without prior induction. However, when induced with 0.1 μg/mL erythromycin, BS-071 average division rates started at 1.8 div/h and decreased to 0.6 div/h indicating higher resistance to clindamycin after induction than susceptible strain BS-042.

3.5. Minimum clones required for classification

MRSA phenotype test results were based on an average total clone count of 324 ± 133 (range = 28–762) clones per test. Computer simulation results showed analysis based on 10 or more clones per test produced 100% sensitivity for MRSA phenotype detection (Fig. 11(a)). Analysis based on 3 to 5 clones per test produced 99% sensitivity, and results from 1 clone per test produced 84% sensitivity. For MSSA phenotype detection, 100% specificity was obtained for all numbers of clones. Clindamycin resistance detection test results were based on an average total clone count of 224 ± 101 (range = 23–655) clones per test. Computer simulation results showed analysis based on 5 or more clones per test produced 95% sensitivity (Fig. 11(b)). Analysis of 3 clones per test produced 96% sensitivity, and analysis of 1 clone per test produced 71% sensitivity. For clindamycin susceptibility detection, analysis based on 10 or more clones per test produced 100% specificity. Analysis of 1 to 5 clones per test produced specificities ranging from 97 to 100%.

3.6. Population analysis profiles by automated microscopy and plating

Population analysis profiles of isolates Mu50, Mu3, 1-6I, 1-4C, BS-003 and 1-3C were generated using automated microscopy and traditional plate-based methods (Fig. 12). Strains 1-3C (vancomycin MIC = 0.5 μg/mL) and BS-003 (vancomycin MIC = 2 μg/mL) showed greater susceptibility to vancomycin than hVISA reference strain Mu3 (vancomycin MIC = 3 μg/mL) by both methods (AUCs = 3.1 and 4.4, respectively, *vs.* 5.1 for Mu3 by the plate method and AUCs = 5.9 and 6.4, respectively, *vs.* 6.7 for Mu3 by automated microscopy), classifying them as VSSA's relative to the Mu3 reference strain. Strain 1-6I (vancomycin MIC = 4 μg/mL) showed greater resistance to vancomycin than VISA reference strain Mu50 (vancomycin MIC = 8 μg/mL) by both methods (AUC = 8.0 *vs.* 5.4 for Mu50 by the plate method and AUC = 8.6 *vs.* 7.9 for Mu50 by automated microscopy). Although strain 1-4C (vancomycin MIC = 0.5 μg/mL) had greater susceptibility to vancomycin than Mu3, its area under the curve was greater than 0.9 times the Mu3 area under the curve (4.9 *vs.* 4.6), classifying it as hVISA by the

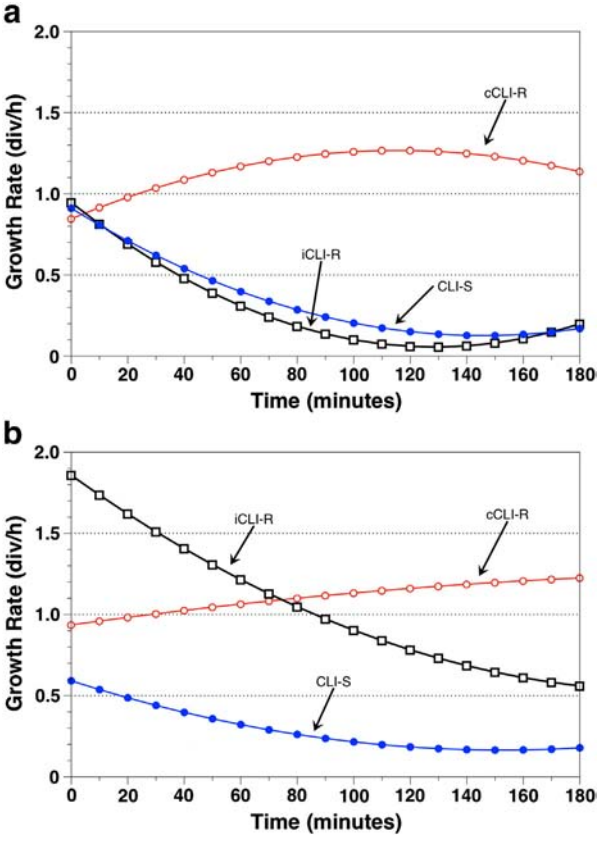

Fig. 10. Growth curves for *S. aureus* strains exhibiting constitutive clindamycin resistance (BS-051, cCLI-R), induced clindamycin resistance (BS-071, iCLI-R), and clindamycin susceptibility (BS-042, CLI-S). The curves are based on the average division rates of all clones in the strain population over 3 h of exposure to 0.5 μg/mL clindamycin following 1 h of exposure to (a) Mueller–Hinton broth or (b) 0.1 μg/mL erythromycin.

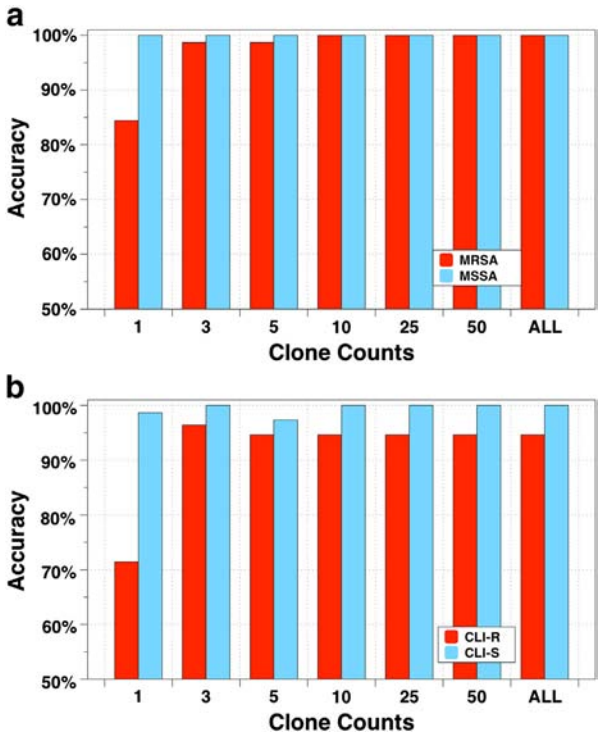

Fig. 11. Sensitivity and specificity by total number of clones analyzed for (a) MRSA phenotype test and (b) clindamycin resistance test. The average growth probabilities of n randomly selected clones from triplicate runs of 131 CDC *S. aureus* isolates were calculated to determine the minimum number of clones required to achieve a result. Y-axis is truncated at 50% to clarify region of difference. CLI-R = clindamycin resistant; CLI-S = clindamycin susceptible.

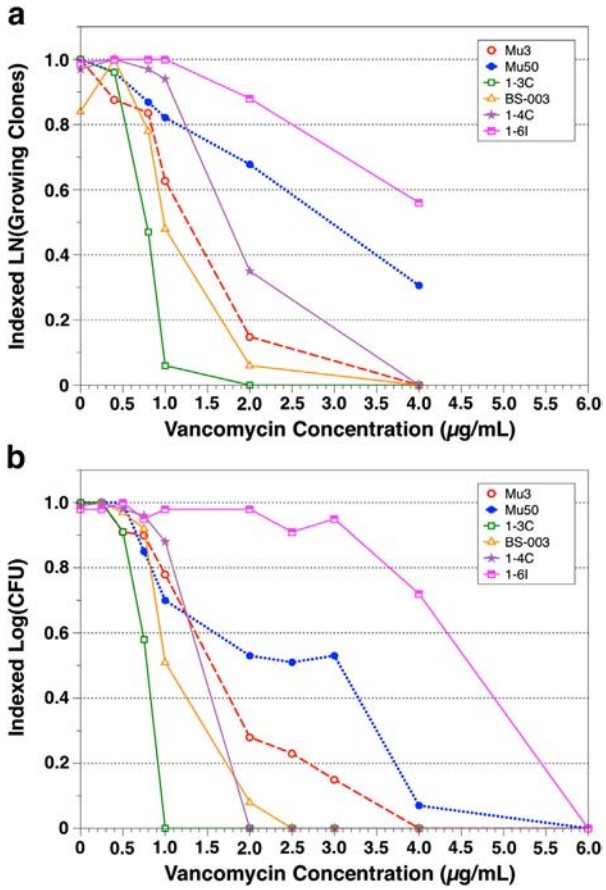

Fig. 12. Population analysis profiles for *S. aureus* isolates Mu50 (ATCC-700699), Mu3 (ATCC-700698), 1-6I, 1-4C, BS-003, and 1-3C with vancomycin MICs of 8, 3, 4, 0.5, 2, and 0.5 μg/mL, respectively, were generated by (a) automated microscopy and (b) traditional plate-based methods using multiple concentrations of vancomycin ranging from 0 to 4 μg/mL for automated microscopy and 0 to 6 μg/mL for the plate method. Counts were normalized and indexed between 0 and 1.

plate-based method (Hiramatsu et al., 1997). 1-4C (AUC = 7.7) showed greater susceptibility to vancomycin than Mu50, but greater resistance than Mu3, classifying it as hVISA by automated microscopy as well. Automated microscopy results were generated from counting the number of growing clones with a 4-fold increase in mass after 4 h of exposure to different concentrations of vancomycin. Images of clone growth in 0 to 4 μg/mL vancomycin at 0, 2 h and 4 h are shown for hVISA reference strain Mu3 (Fig. 13).

4. Discussion

In this study, automated microscopy of immobilized bacterial cells demonstrated the ability to characterize the responses of individual progeny clones within a *S. aureus* sample population. The method was able to use growth data collected over 4 h from as few as 10 growing clones to accurately derive the susceptibility of test isolate classification in multiple concurrent antibiotic tests. None of the studied resistant phenotypes can be reliably performed using direct organism/antibiotic MIC breakpoints: *e.g.* methicillin MIC, clindamycin MIC, or vancomycin MIC (van Hal et al., 2011). These tests therefore presented a stringent challenge. In addition, the strain collection used to challenge the microscopy MRSA assay specifically included isolates that expressed borderline methicillin (oxacillin) susceptibility and resistance. In addition to these results, automated microscopy showed feasibility for directly detecting and characterizing complex modes of resistance expression including heterogeneous response and inducible resistance.

MRSA has long been known to express a high degree of heteroresistance (Tomasz et al., 1991). Automated microscopy showed clear differences in the distribution of clonal growth rates during cefoxitin exposure with different isolates (Fig. 8). Strain BS-001 (Fig. 8(a)) had the MSSA phenotype as determined by cefoxitin disk diffusion (25 mm). A strong and steady shift in clonal growth rates occurred, from normal at 30 min (relative to drug-free growth controls) to lysis (negative growth rate), arrest, or substantially slowed division rate at 180 min, with 27% of clones having division rates greater than zero. At the opposite extreme, BS-006 (Fig. 8(c)) appeared to be a constitutive highly resistant strain (cefoxitin disk zone = 6 mm). During cefoxitin exposure, there was a slight overall rise in clonal growth rates from 30 to 180 min, with a broad distribution at the end. After 180 min, 97% of the BS-006 clone population exhibited division rates greater than zero. In between, BS-067 appeared to express heteroresistance (Fig. 8(b), cefoxitin disk zone = 19 mm). Slightly depressed growth rates at 30 min spread broadly through 180 min with 71% of clones continuing to exhibit positive growth rates despite an overall slowing trend. These results show that automated microscopy can differentiate MSSA and MRSA isolate phenotypic responses after just 3 h of growth compared to 18 h required by current broth microdilution methods.

Another significant finding was direct observation of MRSA induction, which has also long been recognized (Ubukata et al., 1989). Serial cefoxitin induction was used to determine whether a significant induction occurred and, if so, how it might affect assay performance. 2/77 MRSA strains exhibited a significant induction effect. Fig. 9 shows the growth curves for constitutive MRSA BS-006, MSSA BS-002, and inducible MRSA BS-023. Without induction, the BS-023 change in growth rate during 6 μg/mL cefoxitin exposure closely paralleled that of MSSA BS-002. Induction for 1 h with 1 μg/mL cefoxitin substantially shifted the growth curve to closely parallel that of constitutive MRSA BS-006.

Lack of induction could lead to a very major error, identifying a strain as MSSA when in fact it is an inducible MRSA. Although this situation may rarely occur with conventional AST, a recent research report (Penn et al., 2013) suggests that it may occur on occasion. Using direct induction appears to reduce or eliminate this risk. In addition, the strong result of induction may enable a shorter required test time for reliable interpretation rather than extending test duration in the hope of self-induction eventually producing the correct result.

The same rationale and findings apply to inducible clindamycin resistance. Fig. 10 compares the growth curves for constitutive clindamycin resistance (strain BS-051), inducible resistance (BS-071), and susceptibility (BS-042) with and without 0.1 μg/mL erythromycin induction for 1 h. Without induction, BS-071 would have caused a very major error under the conditions that were tested.

Finally, automated microscopy differentiated between VSSA, hVISA, and VISA phenotypes based on accelerated population analysis profiles. The microscopy PAP as with conventional PAP (Hiramatsu et al., 1997) compared the area under a PAP curve to that of the Mu3 (hVISA) reference strain. Fig. 12 shows that microscopy PAP results were analogous to traditional culture results for the same strains.

hVISA strains exhibit vancomycin MICs in the susceptible range and can be missed by standard MIC-based screening methods (Howden et al., 2010). For example, hVISA strain 1-4C had a vancomycin MIC of 0.5 μg/mL by broth microdilution. However, population analysis by culture methods and by automated microscopy both classified it as hVISA (Fig. 12). Traditional agar-dilution PAP culture methods are laborious and require 48 h to produce a result. In this study, traditional agar dilution PAPs required manual plating of eight isolate dilutions on agar plates containing ten different concentrations of vancomycin. In contrast, automated microscopy required testing with ten different vancomycin concentrations, and data collected during 4 h of growth was sufficient to achieve a result.

MRSA phenotype results had no discordances with the cefoxitin disk diffusion reference. There was, however, one discrepancy with *mecA*

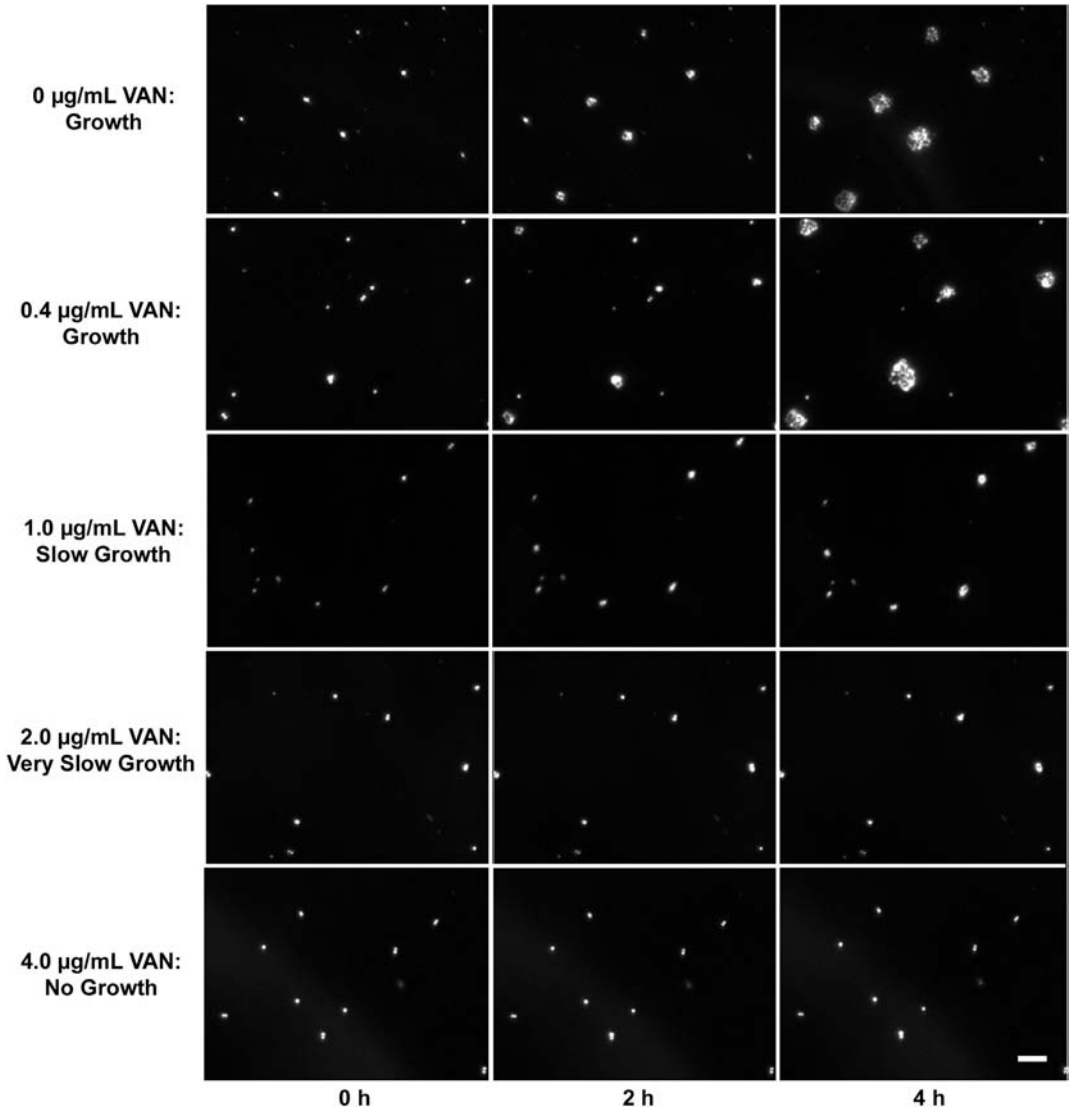

Fig. 13. Dark-field images of hVISA reference strain Mu3 (ATCC 700698) in different vancomycin concentrations (0, 0.4, 1, 2 and 4 µg/mL) at 0, 2 and 4 h. The number of growing clones in each vancomycin concentration after 4 h was used to generate population analysis profiles. Growth was determined by mass increase over time. Images are zoomed in and contrast enhanced for visualization in print. Scale bar in the lower right image is 50 µm.

detection by PCR, which was not the reference used to assess performance. As noted earlier by Swenson et al. (2007), one strain in the CDC collection, BS-089, has a mutated *mecA* as a result. This strain tested as phenotypically susceptible in the earlier study (cefoxitin disk zone 28 mm, cefoxitin MIC 4 µg/mL, and oxacillin MIC 0.5 µg/mL) and by cefoxitin disk diffusion in this study. Unlike the earlier study, this study was not intended to correlate MRSA test results with *mecA* content. The finding in this study supports concerns expressed about gene detection methods that may miss mutated genes, detect other mutations as affirmative as with BS-089, and detect markers from dead bacteria, non-viable bacteria, and cell debris arising from successful antibiotic treatment (Afshari et al., 2012).

Three inducible clindamycin resistant strains tested with induction produced growth probability scores in the susceptible range. Further optimization of the clindamycin resistance assay may be necessary to improve accuracy.

Computer simulations demonstrated that in this study, classifying the phenotypic response of a single clone was enough to predict the response of susceptible isolates, achieving >97% concordance with reference methods. A minimum of 10 clones, however, was required to reliably predict the response of resistant isolates. This finding may reflect the homogeneous nature of susceptible isolate populations in comparison to resistant strains that frequently have subpopulations exhibiting varying levels of resistance.

The use of previously characterized isolates was a limitation of this study. Further studies are warranted for testing a broad collection of clinical isolates, including additional borderline characteristics, and potentially to explore the advantages of direct live-cell extraction and analysis directly to patient specimens.

In conclusion, automated microscopy of immobilized live bacterial cells offers an innovation that can infer the response of an isolate or sample population by using responses from as few as 10 growing clones. It differentiates susceptible from non-susceptible phenotypes within a few hours, and is not confounded by mutations or heterogeneous or inducible resistance phenotypes. In a clinical setting, this method may allow clinicians to choose the right antibiotic sooner in order to successfully treat the most common cause of serious infection presenting to the healthcare setting. It may also be useful for deciphering increasingly complex resistance phenotypes that are not always apparent with current conventional methodology.

Author declarations

Author SM is an employee of Accelerate Diagnostics Inc. Author CSP has received honoraria from Accelerate Diagnostics. Participation by the Denver Health Medical Center was funded by grants from Accelerate Diagnostics to the study site institution and not to investigator CSP or SEK.

Acknowledgments

The authors gratefully acknowledge contributions by the following individuals: Mike Dunne of Washington University for providing potential hVISA strains and for suggesting productive areas for research; Christina Chantell of Accelerate Diagnostics for copywriting, editing, and data review; Jana Swenson and Jean Patel for providing the CDC *S. aureus* reference collection for borderline oxacillin resistance phenotypes and clindamycin resistance variants; and the laboratory staff of Accelr8 Technology Corp. (now Accelerate Diagnostics Inc.).

References

Afshari, A., Schrenzel, J., Ieven, M., Garbarth, S., 2012. Bench-to-bedside review: rapid molecular diagnostics for bloodstream infection — a new frontier? Crit. Care 16, 222.

Chambers, H.F., Deleo, F.R., 2009. Waves of resistance: *Staphylococcus aureus* in the antibiotic era. Nat. Rev. Microbiol. 7, 629–641.

Clinical and Laboratory Standards Institute, 2009. Performance Standards for Antimicrobial Susceptibility Testing; Twenty-third Informational Supplement, M100-S23, Wayne, PA.

Hiramatsu, K., Aritaka, N., Hanaki, H., Kawasaki, S., Hosoda, Y., Hori, S., Fukuchi, Y., Kobayashi, I., 1997. Dissemination in Japanese hospitals of strains of *Staphylococcus aureus* heterogeneously resistant to vancomycin. Lancet 350, 1670–1673.

Howden, B.P., Davies, J.K., Johnson, P.D., Stinear, T.P., Grayson, M.L., 2010. Reduced vancomycin susceptibility in *Staphylococcus aureus*, including vancomycin-intermediate and heterogeneous vancomycin-intermediate strains: resistance mechanisms, laboratory detection, and clinical implications. Clin. Microbiol. Rev. 23, 99–139.

Ibrahim, E.H., Sherman, G., Ward, S., Fraser, V.J., Kollef, M.H., 2000. The influence of inadequate antimicrobial treatment of bloodstream infections on patient outcomes in the ICU setting. Chest 118, 146–155.

Iregui, M., Ward, S., Sherman, G., Fraser, V.J., Kollef, M.H., 2002. Clinical importance of delays in the initiation of appropriate antibiotic treatment for ventilator-associated pneumonia. Chest 122, 262–268.

Klevens, R.M., Morrison, M.A., Nadle, J., Petit, S., Gershman, K., Ray, S., Harrison, L.H., Lynfield, R., Dumyati, G., Townes, J.M., Craig, A.S., Zell, E.R., Fosheim, G.E., McDougal, L.K., Carey, R.B., Fridkin, S.K., 2007. Invasive methicillin-resistant *Staphylococcus aureus* infections in the United States. JAMA 298, 1763–1771.

Landrum, M.L., Neumann, C., Cook, C., Chukwuma, U., Ellis, M.W., Hospenthal, D.R., Murray, C.K., 2012. Epidemiology of *Staphylococcus aureus* blood and skin and soft tissue infections in the US military health system, 2005–2010. JAMA 308, 50–59.

Liu, C., Bayer, A., Cosgrove, S.E., Daum, R.S., Fridkin, S.K., Gorwitz, R.J., Kaplan, S.L., Karchmer, A.W., Levine, D.P., Murray, B.E., Rybak, M.J., Talan, D.A., Chambers, H.F., 2011. Clinical practice guidelines by the Infectious Diseases Society of America for the treatment of methicillin-resistant *Staphylococcus aureus* infections in adults and children: executive summary. Clin. Infect. Dis. 52, 285–292.

Metzger, S., Bergmann, G., Howson, D., Kim, W., Kulprathipanja, N., Mascali, J., Yushkevich, I., 2008. Direct identification of MRSA and MLS_B phenotypes in *Staphylococcus aureus* using small numbers of immobilized cells. Abstr. 108th Gen. Meet. Am. Soc. Microbiol (abstr C-005).

Metzger, S., Price, C.S., Dunne Jr., W.M., Howson, D., 2011. Automated 4-hour detection of heteroresistant vancomycin-intermediate *Staphylococcus aureus* (hVISA). Abstr. 111th Gen. Meet. Am. Soc. Microbiol (abstr C-083).

Muscedere, J., Dodek, P., Keenan, S., Fowler, R., Cook, D., Heyland, D., VAP Guidelines Committee and the Canadian Critical Care Trials Group, 2008. Comprehensive evidence-based clinical practice guidelines for ventilator-associated pneumonia: diagnosis and treatment. J. Crit. Care 23, 138–147.

Penn, C., Moddrell, C., Tickler, I.A., Henthorne, M.A., Kehrli, M., Goering, R.V., Tenover, F.C., 2013. Wound infections caused by inducible methicillin-resistant *Staphylococcus aureus* strains. J. Glob. Antimicrob. Resist. 1, 79–83.

Pfeltz, R.F., Schmidt, J.L., Wilkinson, B.J., 2001. A microdilution plating method for population analysis of antibiotic-resistant *Staphylococci*. Microb. Drug Resist. 7, 289–295.

Skrupky, L.P., Micek, S.T., Kollef, M.H., 2009. Bench-to-bedside review: understanding the impact of resistance and virulence factors on methicillin-resistant *Staphylococcus aureus* infections in the intensive care unit. Crit. Care 13, 222.

Swenson, J.M., Lonsway, D., McAllister, S., Thompson, A., Jevitt, L., Zhu, W., Patel, J.B., 2007. Detection of *mecA*-mediated resistance using reference and commercial testing methods in a collection of *Staphylococcus aureus* expressing borderline oxacillin MICs. Diagn. Microbiol. Infect. Dis. 58, 33–39.

Tomasz, A., Nachman, S., Leaf, H., 1991. Stable classes of phenotypic expression in methicillin-resistant clinical isolates of *Staphylococci*. Antimicrob. Agents Chemother. 35, 124–129.

Ubukata, K., Nonoguchi, R., Matsuhashi, M., Konno, M., 1989. Expression and inducibility in *Staphylococcus aureus* of the *mecA* gene, which encodes a methicillin-resistant *S. aureus*-specific penicillin-binding protein. J. Bacteriol. 171, 2882–2885.

van Hal, S.J., Barbagiannakos, T., Jones, M., Wehrhahn, M.C., Mercer, J., Chen, D., Paterson, D.L., Gosbell, I.B., 2011. Methicillin-resistant *Staphylococcus aureus* vancomycin susceptibility testing: methodology correlations, temporal trends and clonal patterns. J. Antimicrob. Chemother. 66, 2284–2287.

Weisblum, B., Siddhikol, C., Lai, C.J., Demohn, V., 1971. Erythromycin-inducible resistance in *Staphylococcus aureus*: requirements for induction. J. Bacteriol. 106, 835–847.